Journal of Magnetic Resonance **148,** 78–87 (2001)
doi:10.1006/jmre.2000.2205, available online at http://www.idealibrary.com on IDEAL®

Spin-State-Selective Excitation in Selective 1D Inverse NMR Experiments

Teodor Parella*[,1] and Jordi Belloc†

*Servei de Ressonància Magnètica Nuclear, Universitat Autònoma de Barcelona, Bellaterra, Barcelona E-08193, Spain; and †Laboratoris Uriach, Degà Bahí 59, E-08026 Barcelona, Spain

Received May 15, 2000; revised August 7, 2000

A general and very simple strategy for achieving clean spin-state-selective excitation with full sensitivity in carbon-selective gradient-enhanced 1D HMQC and HSQC pulse schemes is presented. The incorporation of an additional hard 90° ^{13}C pulse applied along a specific orthogonal axis just prior to acquisition into the conventional sequences allows us to select a simultaneous coherence transfer pathway which usually is not detected. The superimposition of this resulting antiphase magnetization to the conventional in-phase magnetization gives the exclusive excitation of the directly attached proton showing only the α or β spin state of the passive ^{13}C nucleus. The propagation of this particular spin state to other protons can be accomplished by adding any homonuclear mixing process just after this supplementary pulse. Such an approach affords a suite of powerful selective 1D ^{13}C-edited NMR experiments which are helpful for resonance assignment purposes in overcrowded proton spin systems and also for the accurate determination of the magnitude and sign of long-range proton–carbon coupling constants in CH spin sytems for samples at natural abundance. Such measurements are performed by measuring the relative displacement of relayed signals in the corresponding α and β 1D subspectra.

Key Words: **NMR; spin-state-selective excitation; long-range proton–carbon coupling constants; selective experiments; pulsed field gradients.**

INTRODUCTION

Spin-state-selective (S^3) pulse schemes that manipulate the coherences exclusively belonging to the α or β state of a particular coupling pattern have been successfully applied in biomolecular NMR. For instance, coupling constants can be measured with high accuracy from multidimensional NMR experiments based on the generation of two separate subspectra with each displaying only one multiplet component of a doublet. Applications have been reported for the determination of homonuclear (*1–3*), heteronuclear (*1, 4*), through-hydrogen-bond (*5, 6*), and residual dipolar (*7–10*) coupling constants. On the other hand, the selection of the slowest relaxing component of a multiplet improves the sensitivity and resolution of multidimensional NMR experiments of large biomolecules in high magnetic fields by applying the well-known TROSY approach (*11*). Other applications of the S^3 principle have been demonstrated for the suppression of diagonal peaks in multidimensional spectra (*12, 13*) or the sensitivity improvements achieved in INADEQUATE experiments (*14*).

Selective S^3 excitation has been also achieved in carbon-selective 1D inverse experiments by applying an specific selective carbon pulse on a particular satellite line or a proper combination of delay and offset settings. Such an approach has been applied to measure precise long-range proton–carbon coupling constants for samples at natural abundance (*15–21*) by appending a TOCSY transfer step after achieving the selective S^3 excitation and recording two separate 1D subspectra, one for the α state and one for the β state. Thus, coupling constants even smaller than the linewidth can be direclty measured by comparing the relative displacement of the 1D TOCSY multiplets.

In this work we show that a very simple modification of the previously reported gradient-enhanced 1D HMQC and HSQC pulse sequences (*22–27*) achieves clean selective S^3 excitation without needing to apply extra selective pulses or considering appropiate delays and offset settings. The proposed idea is based in the original works of Sorensen *et al.* (*1*) and Ross *et al.* (*28*). The incorporation of a single hard 90° ^{13}C pulse (referred to as the S^3 pulse) applied from a specific orthogonal axis just prior to acquisition selects a simultaneous coherence transfer pathway (CTP) which usually is not detected. The superimposition of this resulting antiphase magnetization to the conventional in-phase magnetization gives the exclusive excitation of the directly attached proton showing only the α or β spin state of the passive ^{13}C nucleus with full sensitivity. In fact, this approach is a reduced version of the well-known PEP methodology (*29*) in which the second retro-INEPT (*25*) is limited to a single carbon pulse. The extension of this simple strategy to analogs pseudo-3D experiments allows the accurate determination of long-range proton–carbon coupling constants on protonated carbons by directly measuring the displacement of signals in the corresponding two 1D subspectra.

[1] To whom correspondence should be addressed.

1090-7807/01 $35.00

RESULTS AND DISCUSSION

The basic pulse schemes of carbon-selective 1D α/β-HMQC and α/β-HSQC experiments are despicted in Fig. 1, in which the only novelty with respect to the original sequences is the inclusion of the mentioned S^3 pulse with phase ϕ.

As predicted theoretically, both pulse sequences offer similar experimental sensitivity ratios and they are easily analyzed and understood in terms of shift product operators (*30*),

$$I^{\pm} = I_x \pm iI_y, \qquad [1]$$

in which I^+ corresponds to a coherence order $p = +1$, whereas I^- corresponds to a coherence order $p = -1$. The 90° and 180° pulse effects and the evolution under J coupling are the only basic transformations to consider. Otherwise, chemical shift evolution can be neglected because offsets are set on the selected resonances during all experiments. The crucial point of the strategy described in this work relies on the effect of a 90° S pulse applied along an axis ϕ on a mixture of DQC and ZQC as shown in Eqs. [2a–2c].

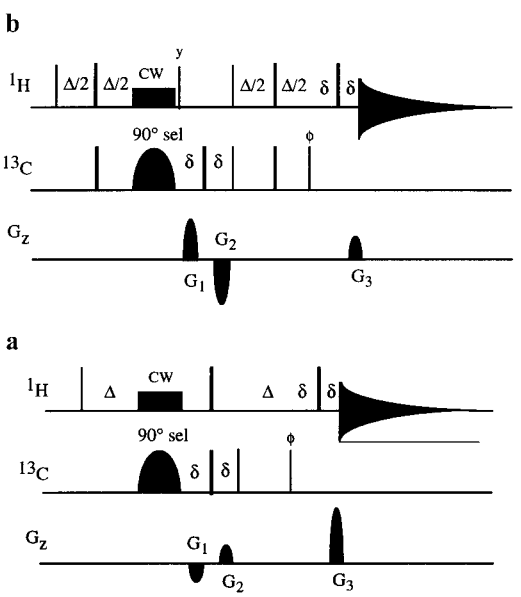

FIG. 1. Selective gradient-enhanced carbon-selective 1D (a) α/β-HMQC and (b) α/β-HSQC pulse schemes. Hard 90° and 180° pulses are indicated by vertical narrow and wide black bars. A selective 90° carbon pulse is indicated by a shaded shape. Proton decoupling during the selective carbon pulse is achieved by applying a simultaneous 3-kHz continuous wave (CW) period. All pulses are applied from the x axis unless otherwise indicated. A minimum two-step phase cycle was applied in which the selective carbon 90° pulse and the receiver are inverted on alternate scans. The interpulse delay, Δ, is optimized to $1/(2*{}^1J_{CH})$. Gradients of duration (δ) of 1 ms, with a recovery time of 100 μs and maximum strength of 50 G/cm, are also indicated by shaded shapes on the line G_z. Proton and carbon offsets are set on resonance of the selected proton and carbon signals through all experiments. See text for discussion about the phase ϕ and gradient ratios.

$$I^+(S^+ + S^-) \xrightarrow{90^S_X} I^+(S^+ + S^-) \qquad [2a]$$

$$I^+(S^+ + S^-) \xrightarrow{90^S_Y} 2I^+S_z \qquad [2b]$$

$$I^+(S^+ + S^-) \xrightarrow{90^S_{-Y}} -2I^+S_z \qquad [2c]$$

Spin-selective states are defined using single-transition operators (I^-S^α and I^-S^β) which are best described as the sum or difference of in-phase and antiphase magnetization.

$$I^-S^\alpha = I^- + 2I^-S_z \qquad [3a]$$

$$I^-S^\beta = I^- - 2I^-S_z \qquad [3b]$$

Analyzing both sequences of Fig. 1, the following coherences are present just before the S^3 pulse:

$$\frac{-i}{4}(I^+ + I^+S^+ + I^+S^-). \qquad [4]$$

The first term stands for conventional in-phase magnetization whereas the second and third terms represent DQ and ZQ coherences, respectively. These multiple-quantum coherences (MQC) are usually not observed but can be converted to detectable magnetization by applying the PEP methodology, in other words by repeating the same spin manipulation but from an orthogonal axis (*29*). Considering Eqs. [2a–2c], the simple choice of the phase ϕ of this additional S^3 pulse allows us to obtain the conventional large in-phase doublet due to $^1J_{CH}$ if it is applied along the x axis,

$$\xrightarrow{90^S_X - \delta - 180^I_X - \delta} \frac{-i}{4} I^-, \qquad [5a]$$

or the corresponding α or β multiplet component if it is applied from the y or $-y$ axis, respectively,

$$\xrightarrow{90^S_Y - \delta - 180^I_X - \delta} \frac{-i}{4}(I^- + 2I^-S_z) = \frac{-i}{4} I^-S^\alpha \qquad [5b]$$

$$\xrightarrow{90^S_{-Y} - \delta - 180^I_X - \delta} \frac{-i}{4}(I^- - 2I^-S_z) = \frac{-i}{4} I^-S^\beta. \qquad [5c]$$

Other interesting advantages of the proposed experiments

are that selective S^3 excitation is achieved without needing extra selective pulses or changing offsets during the sequence, there are no special data processing requirements, and maximum sensitivity with high spectral quality is always obtained under standard conditions.

α/β-HMQC EXPERIMENT

The first approach is a simple modification of the selective ge-1D HMQC experiment (*21–23*), in which the first 90 ^{13}C pulse is applied selectively on the target carbon (Fig. 1a). After this pulse, MQCs are labeled with two dephasing gradients inserted into a heteronuclear spin echo in order to avoid proton and carbon chemical shifts evolution. These MQCs are represented as

$$\frac{i}{2}(I^+ + I^-)(S^+ - S^-). \qquad [6]$$

The general equation for gradient refocusing in this experiment can be written as

$$(4p_{1,\mathrm{H}} + p_{1,\mathrm{C}})G_1 + (4p_{2,\mathrm{H}} + p_{2,\mathrm{C}})G_2 - 4G_3 = 0, \qquad [7]$$

where $p_{i,j}$ define the selected coherence order p during the gradient i and for the nucleus j. Several gradient ratios can be chosen depending on whether DQC or ZQC are retained during the defocusing G_1 and G_2 gradients (Table 1).

In the following, we assume that the following pathway is selected by a $-2{:}2{:}5$ gradient ratio although all other options give the same final results.

$$\frac{-i}{2} I^- S^- \xrightarrow{180^I_X/180^S_X} \frac{-i}{2} I^+ S^+. \qquad [8]$$

A hard 90_x ^{13}C pulse generates antiphase SQ proton coherences which evolve during a free Δ evolution period in order to obtain the conventional in-phase proton magnetization.

TABLE 1
Gradient Ratios to Achieve Coherence Selection in α/β-HMQC-like Experiments

$G_1{:}G_2{:}G_3$ ratio	CTP selected during G_1	CTP selected during G_2
$2{:}-2{:}5$	I^+S^+	I^-S^-
$-2{:}2{:}5$	I^-S^-	I^+S^+
$2{:}-2{:}3$	I^+S^-	I^-S^+
$-2{:}2{:}3$	I^-S^+	I^+S^-

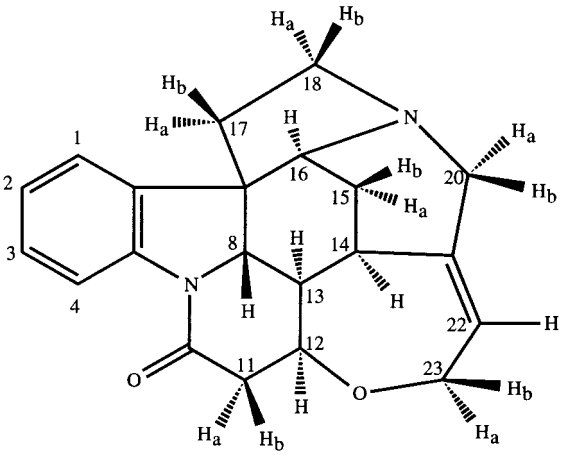

1

However, other undetectable terms are presents in this point as described in Eq. [4]. Thus, the application of another 90° ^{13}C pulse (the S^3 pulse) can convert the remaining MQCs to antiphase proton magnetization whereas the above mentioned in-phase proton magnetization would remain unaffected (see Eqs. [5a–5c]). In any case, a final refocusing G_3 gradient must be inserted into a spin-echo period in order to refocus only the desired proton magnetization which must be detected without ^{13}C decoupling. The result is a clean 1D proton spectrum only displaying one or both ^{13}C satellites due to $^1J_{\mathrm{CH}}$ of the chosen carbon signal where the central and strong ^{1}H–^{12}C signal and other artifacts are efficiently suppressed by the effect of the gradients. Figure 2 shows the experimental results obtained after selectively pulsing the C-12 resonance of strychnine, **1**. Clean in-phase excitation is achieved by setting the phase ϕ of the S^3 pulse to x (Fig. 2c). In this case, a sensitivity decrease by a factor of 2 is achieved at the expense of improved quality when compared to an analog phase-cycle experiment (Fig. 2b) because only a single CTP is selected. Of course, the same result is obtained if the S^3 pulse is omitted.

On the other hand, α or β spin states are exclusively selected by setting ϕ to y or $-y$, respectively, and the sensitivity of the experiment is improved by a factor of 2 by the coaddition of the two contributed CTPs (Figs. 2d and 2e).

α/β-HSQC EXPERIMENT

The same modification described above can be also applied for the regular HSQC pulse train (*21–23*), as shown in Fig. 2b. In fact, this sequence can be regarded as a carbon-selective version of the experiment described in Ref. (*28*). During the defocusing gradi-

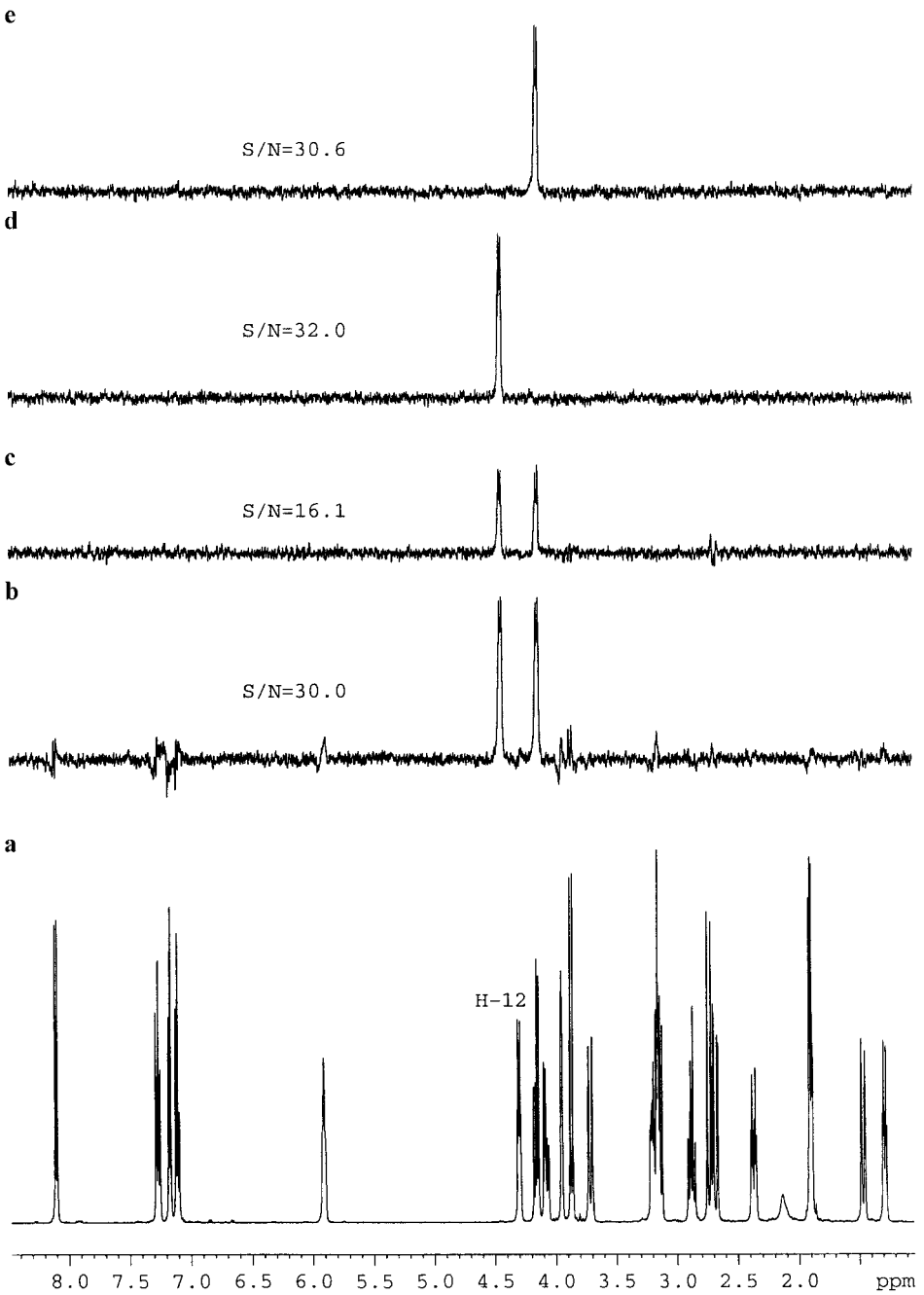

FIG. 2. The 500.13 MHz ^{1}H spectra of strychnine in $CDCl_3$. (a) Conventional; (b) phase-cycled selective 1D HMQC using a BIRD cluster followed by a 400-ms recovery delay to minimize unwanted ^{1}H–^{12}C magnetization (*31*); (c–e) selective ge-1D α/β-HMQC acquired with the pulse sequence of Fig. 1a using $\phi = x, y, -y$, respectively. All spectra have been recorded in a AVANCE 500 Bruker spectrometer equipped with a triple-resonance inverse probehead incorporating a *Z*-gradient coil. The following experimental conditions were applied: relaxation delay of 1 s, interpulse delay of $\Delta = 3.3$ ms, 16 transients with two dummy scans, and a 12-ms selective 90° carbon pulse with a gaussian shape applied on the C-12 carbon resonance. The experimental signal-to-noise ratio is displayed for each spectrum.

ents, antiphase carbon magnetization is present in the form of

$$-I_z(S^+ - S^-). \qquad [9]$$

In this case, the refocusing condition is fullfilled when

$$G_1 p_{1,C} + G_2 p_{2,C} - 4G_3 = 0. \qquad [10]$$

TABLE 2
Gradient Ratios to Achieve Coherence Selection in α/β-HSQC-like Experiments

G_1:G_2:G_3 ratio	CTP selected during G_1	CTP selected during G_2
2:−2:1	I_zS^+	I_zS^-
−2:2:1	I_zS^-	I_zS^+

Two equivalent options for coherence selection are possible (Table 2). Assuming that the following CTP is selected,

$$-I_zS^+ \xrightarrow{180_X^S} -I_zS^-, \qquad [11]$$

a behavior similar to that described for the α/β-HMQC experiment is obtained when simultaneous 90° pulses are applied to both nuclei. Thus, in addition to the conventional antiphase proton magnetization, MQCs are also created although they are not detected under standard conditions.

$$-I_zS^- \xrightarrow{90_X^I/90_X^S} \frac{-i}{4}(I^-S^+ + I^-S^- + 2iS_zI^-)$$

$$\xrightarrow{\Delta/2 - 180_X^{I,S} - \Delta/2} \frac{-i}{4}(I^+S^- + I^+S^+ + I^+) \qquad [12]$$

As found for the HMQC counterpart, the phase ϕ of the S^3 pulse offers the three possiblities described in Eqs. [5a–5c]. Figures 5b–5d show the α/β-HSQC spectra after select the C4 resonance. Although the same sensitivity ratios may be obtained using both HMQC and HSQC sequences, we have experimentally found that the HMQC experiment offers slightly improved sensitivity, possibly due to fewer pulses involved and, therefore, the experiment should be more tolerant to pulse miscalibrations and imperfections.

α/β-PSEUDO-3D EXPERIMENTS

The in-phase character of the detected signal with respect to all homonuclear proton–proton couplings in both α/β-HMQC and α/β-HSQC schemes becomes suitable for introducing any homonuclear mixing process, just between the S^3 pulse and the last spin-echo period (Fig. 3). In other words, the simple incorporation of the S^3 pulse in all pseudo-3D pulse sequences reported in Ref. (*24*) affords a suite of interesting NMR methodologies for the measurement of long-range proton–carbon coupling constants for samples at natural abundance. Such experiments also retain all interesting features of the original sequences for resonance assignment purposes. In addition to the use of the already proposed TOCSY transfer, such measurements could be also succesfully performed using COSY-type and NOE-based building blocks as homonuclear mixing processes. An important point to mention is that all experimental aspects described above for the α/β-HMQC and α/β-HSQC experiments, such as parameter settings, gradient ratios, or the effect of the phase ϕ of the S^3 pulse remain exactly the same and, therefore, such experiments can be defined for general use.

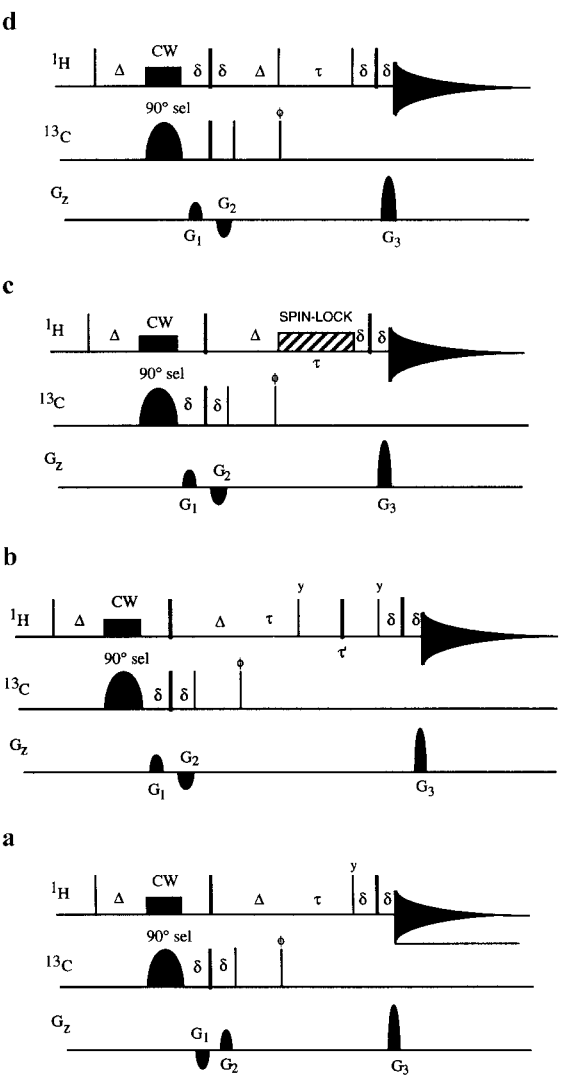

FIG. 3. General schemes for selective gradient-enhanced carbon-selective 1D (a) α/β-HMQC-COSY, (b) α/β-HMQC-RELAY, (c) α/β-HMQC-TOCSY (or also α/β-HMQC-ROESY), and (d) α/β-HMQC-NOESY experiments. The τ and τ' delays are optimized as a function of J_{HH}. A 8-kHz MLEV-16 pulse train was used as a spin-lock for TOCSY transfer and a 3-kHz CW pulse for ROESY transfer in sequence c. All other details are as described in the legend to Fig. 1.

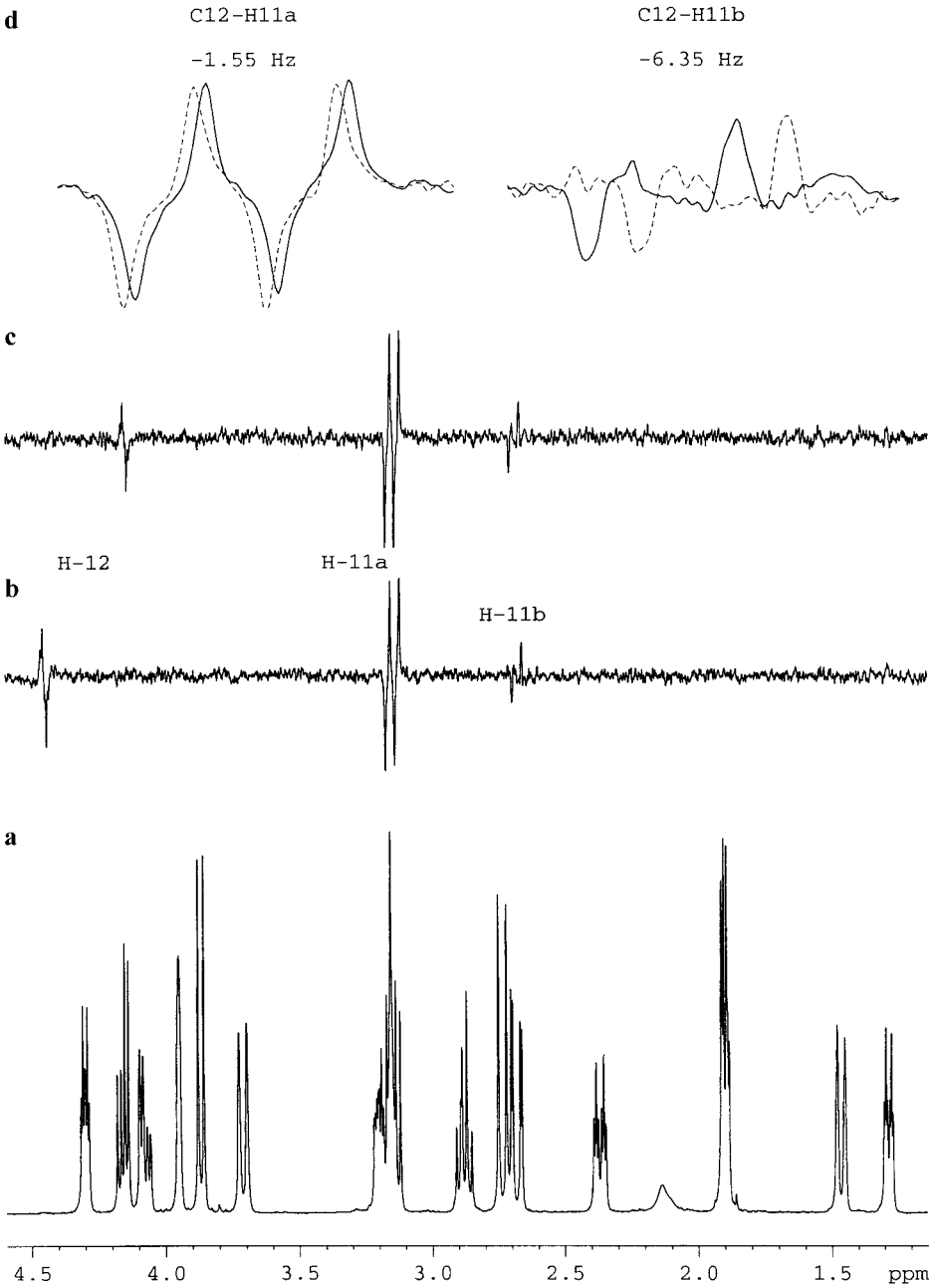

FIG. 4. (b–c) α/β-HMQC-COSY spectra after selectively pulsing on the C-12 resonance. A total of 128 scans have been recorded with two dummy scans for each spectrum using a COSY interpulse delay (τ) of 50 ms. All of the other experimental parameters are as described in the legend to Fig. 2. (d) Expansions of COSY multiplets.

Figure 3a shows the corresponding α/β-HMQC-COSY pulse sequence in which a delay (τ)–90_y(^{1}H) block has been inserted just after the S^3 pulse. The result is a typical ^{13}C-selective-edited COSY spectrum in which 1D COSY peaks appear, showing the characteristic antiphase pattern with respect to the active homonuclear coupling with the directly attached proton (Figs. 4b and 4c). As an additional feature, all COSY signals have also encoded a particular spin state of the target carbon nucleus as a function of the chosen ϕ value. For instance, in the case of $\phi = y$ the transfer mechanism can be summarized as

$$I_1^+ S^\alpha \xrightarrow{\tau} 2I_1^+ I_{2z} S^\alpha \xrightarrow{90_y^I} 2I_{1z} I_2^+ S^\alpha \xrightarrow{\delta - 180_X^I - \delta} 2I_{1z} I_2^- S^\alpha. \quad [13]$$

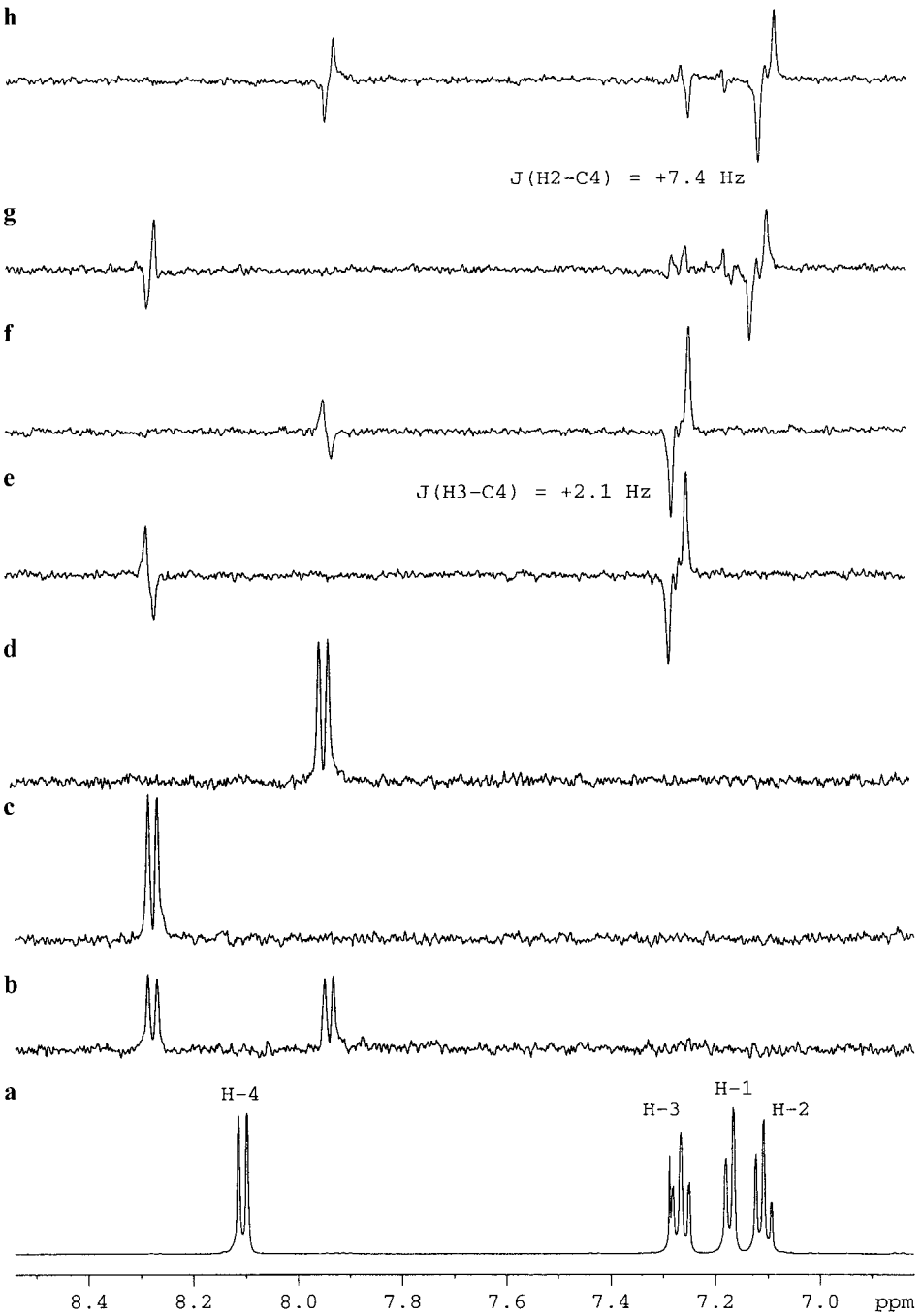

FIG. 5. α/β-HSQC-type spectra after selectively pulsing on the C-4 resonance. (b–d) α/β-HSQC spectra recorded using the pulse sequence of Fig. 1b, using a phase $\phi = x, y$, and $-y$, respectively. The interpulse delay (Δ) was set to 3 ms. (e–f) α/β-HSQC-COSY spectra using an interpulse delay (τ) of 50 ms. A total of 128 scans have been recorded with two dummy scans for each spectrum. (g–h) One-step α/β-HSQC-RELAY spectra using $\tau = 50$ ms and $\tau' = 60$ ms. A total of 512 scans have been recorded with two dummy scans for each spectrum. All other experimental parameters are as described in the legend to Fig. 2.

The relative displacement between the α- and β-relayed signals in the two separate 1D spectra affords the exclusive measurement of the corresponding two-bond proton–carbon coupling constants (Fig. 4d). Furthermore, the sense of this displacement is an indication of the sign of the measured coupling constant. Thus, positive values are due to displacement in the same sense as the large one-bond coupling, whereas opposite sense is found for negative values. Note that the antiphase character of COSY signals is not a disturbance for such a measurement. Similar results are also obtained from the related α/β-HSQC-COSY spectra, as shown in Figs. 5e and 5f.

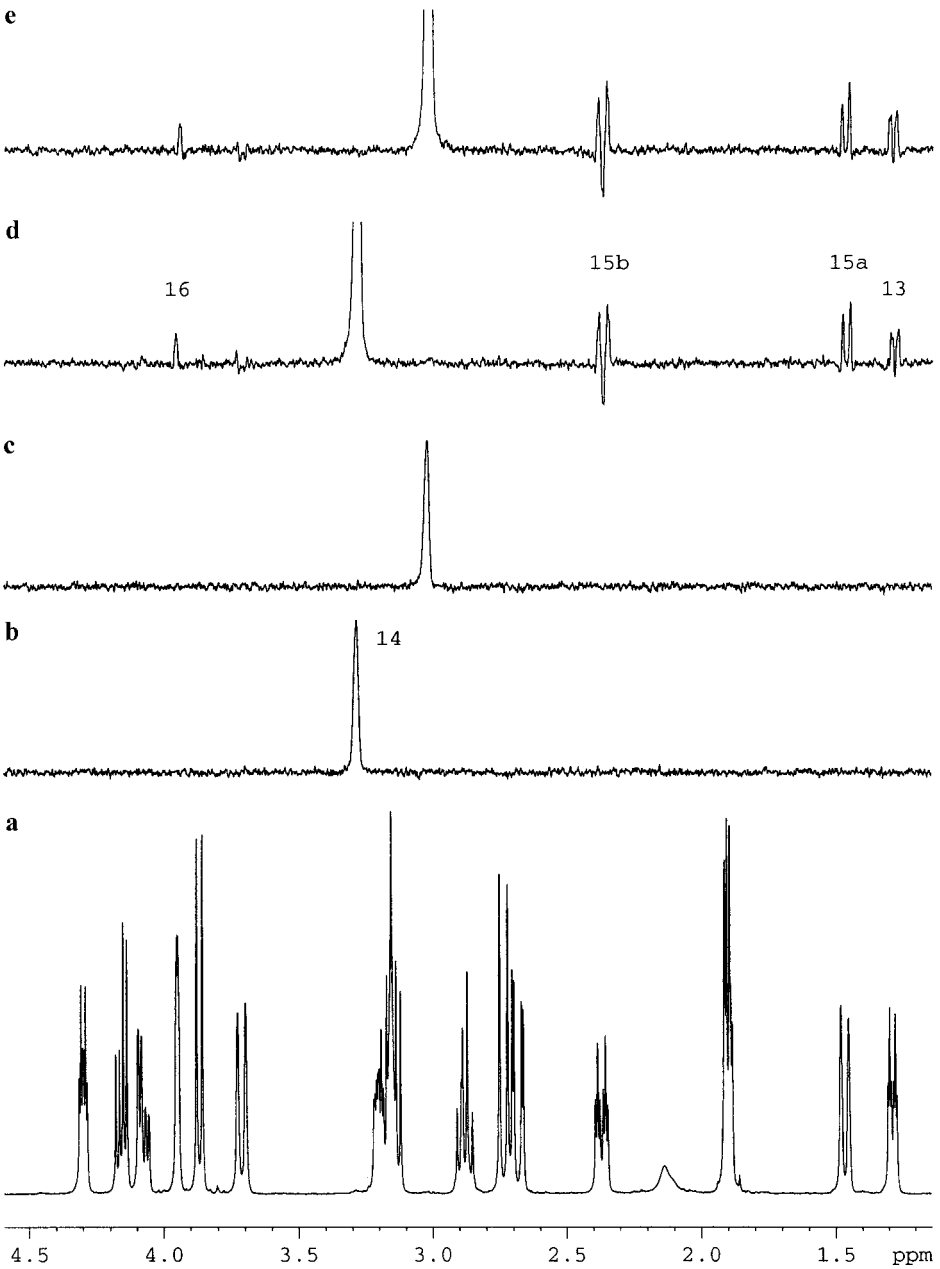

FIG. 6. (b–c) α/β-HMQC spectra after selectively pulsing on the C-14 resonance, using a phase $\phi = y$ and $-y$, respectively. (d–e) α/β-HMQC-TOCSY spectra with a 50-ms mixing time using the scheme of Fig. 2c. The interpulse delay (Δ) was set to 3.6 ms. A total of 256 scans have been recorded with two dummy scans for each spectrum. Other experimental parameters are as described in Fig. 2.

In a similar way, multiple RELAY steps could be added by concatenating additional COSY blocks. Thus, one-step α/β-HMQC-RELAY (Fig. 3b) and α/β-HSQC-RELAY experiments would afford three-bond proton–carbon coupling constants. For instance, Figs. 5g and 5h show how the α/β-HSQC-RELAY spectra, after selectively pulsing the C-4 aromatic carbon, allow the unambiguous measurement of the value and the sign of the ^3J(C4–H2) coupling constant.

However, an in-phase TOCSY-like transfer can be most suitable for transferring magnetization via J. Figure 3c shows the equivalent α/β-HMQC-TOCSY pulse sequence in which a MLEV-16 isotropic mixing sequence is appended after the S^3 pulse. Figure 6 shows the clean spectra obtained after apply it on the C-14 resonance and Fig. 7 shows the corresponding multiplet expansions. Equivalent results are obtained using the α/β-HSQC-TOCSY experiment, as demonstrated for the C-4 resonance in Fig. 8. In this case even the small four-bond coupling constant between C-4 and H-1 is measured with high accuracy from the in-phase multiplets.

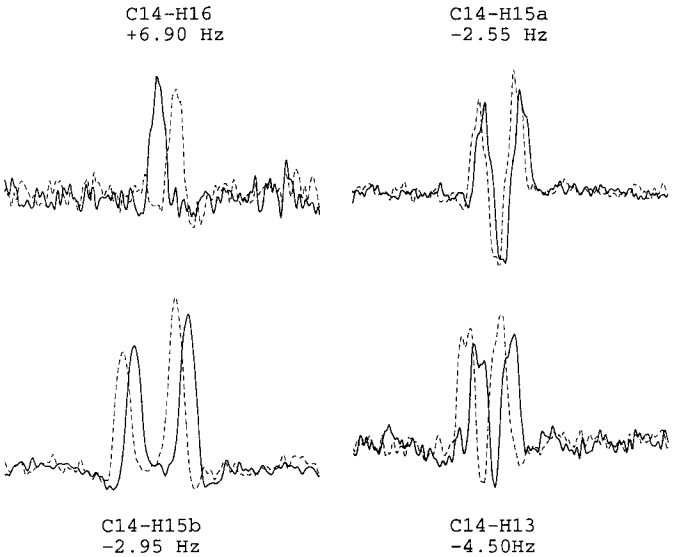

FIG. 7. Expansions of spectra d and e of Fig. 6.

$$I_1^+ S^\alpha \xrightarrow{\text{SL}} I_2^+ S^\alpha \xrightarrow{\delta - 180^I_X - \delta} I_2^- S^\alpha \quad [14]$$

It should also be possible to design new approaches for measuring proton–carbon coupling constants in systems where propagation via homonuclear *J* coupling constants is not efficient by using a ROESY (Fig. 3c) or NOESY (Fig. 3d) building block. The resulting experiment could be also used to measure such coupling values in HC*X*C spin systems where *X* should be a quaternary carbon or a heteronucleus, such as oxygen or nitrogen, as those found through glycosidic linkages in polysaccharides or nucleotides. However, the use of long mixing times in such experiments would afford undesired signal losses basically due to diffusion effects.

CONCLUDING REMARKS

In conclusion, a straightforward way to achieve clear S^3 excitation for *IS* spin systems in selective 1D inverse experiments without needing to include extra requirements for data

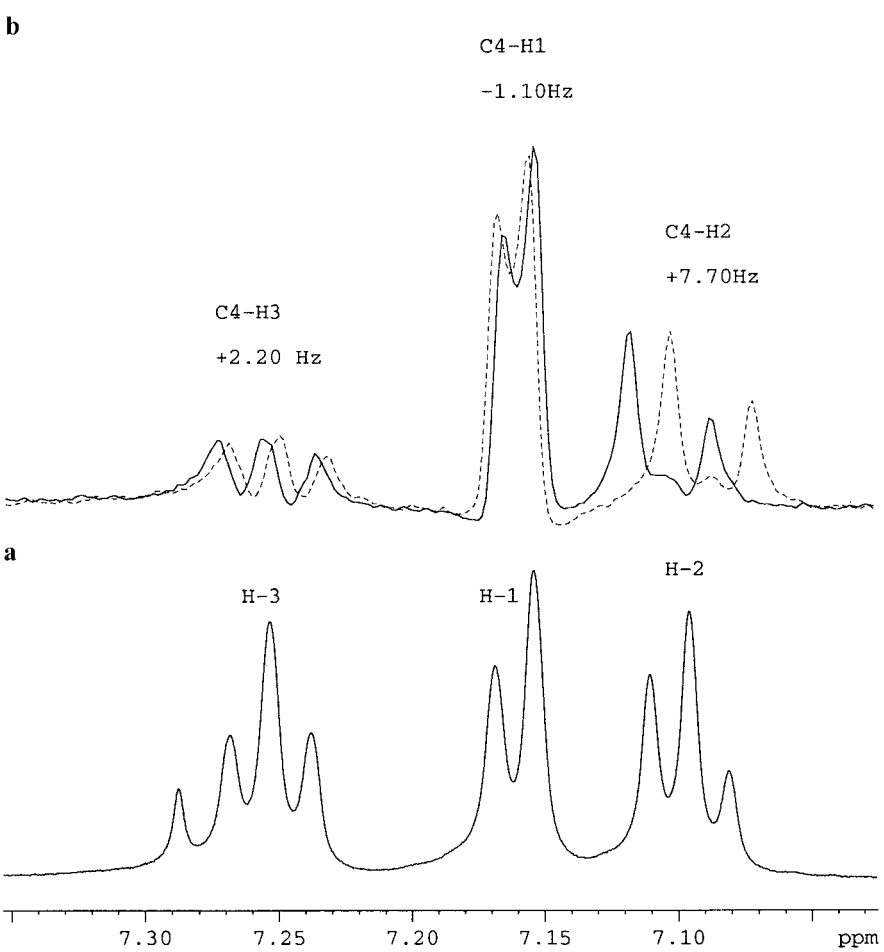

FIG. 8. Expansion of the aromatic part of the α/β-HSQC-TOCSY experiment under the same conditions as described in legend to Fig. 5. The TOCSY mixing time was set to 65 ms.

acquisition or data processing with respect to conventional experiments has been described. Measurement of long-range proton–carbon coupling constants even smaller than the linewidth with high precission has been carried out with simplicity for samples at natural abundance using different pulse schemes. Simultaneous extraction of the magnitude and the sign of these coupling constants is performed by direct analysis of multiplet displacements in 1D spectra without regard to the in-phase or antiphase coupling pattern of the analyzed multiplet and without needing of extra fitting procedures.

ACKNOWLEDGMENTS

Financial support for this research provided by DGES (Project PB98-0914) is gratefully acknowledged. We thank the Servei de Ressonància Magnètica Nuclear, UAB, for allocating instrument time to this project.

REFERENCES

1. M. D. Sorensen, A. Meissner, and O. W. Sorensen, Spin-state-selective coherence transfer via intermediate states of two-spin coherence in IS spin systems. Application to E.COSY-type measurement of J couplings, *J. Biomol. NMR* **10,** 181–186 (1997).
2. A. Meissner, J. O. Duus, and O. W. Sorensen, Spin-state-selective excitation. Application for E.COSY-type measurement of JHH coupling constants, *J. Magn. Reson.* **128,** 92–97 (1997).
3. M. D. Sorensen, A. Meissner, and O. W. Sorensen, ^{13}C natural abundance S^3E and S^3CT experiments for measurement of J coupling constants between ^{13}Ca or ^{1}Ha and other protons in a protein, *J. Magn. Reson.* **137,** 237–242 (1999).
4. A. Meissner, J. O. Duus, and O. W. Sorensen, Integration of spin-state-selective excitation into 2D NMR correlation experiments with heteronuclear ZQ/2Q π rotations for $^{1}J_{XH}$-resolved E.COSY-type measurement of heteronuclear coupling constants in proteins, *J. Biomol. NMR* **10,** 89–94 (1997).
5. A. Meissner and O. W. Sorensen, New techniques for the measurement of C′N and $C'H^N$ J coupling constants across hydrogen bonds in proteins, *J. Magn. Reson.* **143,** 387–390 (2000).
6. A. Meissner and O. W. Sorensen, ^{3h}J coupling between C^α and H^N across hydrogen bonds in proteins, *J. Magn. Reson.* **143,** 431–434 (2000).
7. M. Ottiger, F. Delaglio, and A. Bax, Measurement of *J* and dipolar couplings from simplified two-dimensional NMR spectra, *J. Magn. Reson.* **131,** 373–378 (1998).
8. P. Andersson, K. Nordstrand, M. Sunnerhagen, E. Liepinsh, I. Turovskis, and G. Otting, Heteronuclear correlation experiments for the determination of one-bond coupling constants, *J. Biomol. NMR* **11,** 445–450 (1998).
9. M. H. Lerche, A. Meissner, F. M. Poulsen, and O. W. Sorensen, Pulse sequences for measurement of one-bond ^{15}N–^{1}H coupling constants in the protein backbone, *J. Magn. Reson.* **140,** 259–263 (1999).
10. P. Andersson, J. Weigelt, and G. Otting, Spin-state selection filters for the measurement of heteronuclear one-bond coupling constants, *J. Biomol. NMR* **12,** 435–441 (1998).
11. K. Pervushin, R. Riek, G. Wider, and K. Wuthrich, Attenuated T_2 relaxation by mutual cancellation of dipole–dipole coupling and chemical shift anisotropy indicates an avenue to NMR structures of very large biological macromolecules in solution, *Proc. Natl. Acad. Sci. USA* **94,** 12366–12371 (1997).
12. A. Meissner and O. W. Sorensen, Suppression of diagonal peaks in TROSY-type ^{1}H NMR NOESY spectra of ^{15}N-labeled proteins, *J. Magn. Reson.* **140,** 499–503 (1999).
13. K. V. Pervushin, G. Wider, R. Riek, and K. Wuthrich, The 3D NOESY-[^{1}H–^{15}N]-ZQ TROSY NMR experiment with diagonal peak suppression, *Proc. Natl. Acad. Sci. USA* **96,** 9607–9612 (1999).
14. N. C. Nielsen, H. Thogersen, and O. W. Sorensen, Doubling the sensitivity of INADEQUATE for tracing out the carbon skeleton of molecules by NMR, *J. Am. Chem. Soc.* **117,** 11365–11366 (1995).
15. L. Poppe, S. Sheng, and H. van Halbeek, Stereospecific assignment of exocyclic methylene protons in panose by ^{13}C-filtered 1D TOCSY, *Magn. Reson. Chem.* **32,** 97–100 (1994).
16. R. Bazzo, G. Barbato, and D. O. Cicero, Accurate measurement of heteronuclear long-range coupling constants from 1D subspectra in crowded spectral regions, *J. Magn. Reson. A* **117,** 267–271 (1995).
17. T. Facke and S. Berger, α-β-ge-SELINCOR-TOCSY, a new method for the determination of H, C coupling constants, *J. Magn. Reson. A* **119,** 260–263 (1996).
18. D. yang and K. Nagayama, A sensitivity-enhanced method for measuring heteronuclear long-range coupling constants from the displacement of signals in two 1D subspectra, *J. Magn. Reson. A* **118,** 117–121 (1996).
19. E. Fikushi and J. Kawabata, Heteronuclear long-range couplings from displacement of signals in two 1D subspectra, *J. Magn. Reson. A* **108,** 103–105 (1994).
20. J. M. Nuzillard and R. Freeman, A new route to long-range ^{13}C–^{1}H couplings, *J. Magn. Reson. A* **110,** 262–265 (1994).
21. G. Xu and J. S. Evans, Determination of long-range J_{XH} couplings using excitation-sculpting gradient-enhanced heteronuclear correlation experiments, *J. Magn. Reson. A* **123,** 105–110 (1996).
22. T. Parella, High-quality 1D spectra by implementing pulsed-field gradients as the coherence pathway selection procedure, *Magn. Reson. Chem.* **34,** 329–347 (1996).
23. T. Parella, F. Sánchez-Ferrando, and A. Virgili, Selective gradient-enhanced inverse experiments, *J. Magn. Reson. A* **112,** 106–108 (1995).
24. T. Parella, F. Sánchez-Ferrando, and A. Virgili, Improved HMQC-type and HSQC-type 1D spectra using pulsed field gradients, *J. Magn. Reson. A* **114,** 32–38 (1995).
25. T. Parella, F. Sánchez-Ferrando, and A. Virgili, Sensitivity improvements in selective ^{1}H–^{13}C 1D polarization-transfer schemes, *J. Magn. Reson.* **126,** 278–282 (1997).
26. J. Stelten and D. Leibfritz, Highly selective 1D CH correlations, *Magn. Reson. Chem.* **33,** 827–830 (1995).
27. T. Fäcke and S. Berger, Gradient-enhanced SELINCOR for selective excitation in a ^{13}C-resolved COSY experiment, *Magn. Reson. Chem.* **33,** 144–148 (1995).
28. A. Ross, M. Czisch, and T. A. Holak, Selection of simultaneous coherence pathways with gradient pulses, *J. Magn. Reson. A* **118,** 221–226 (1996).
29. A. G. Palmer III, J. Cavanagh, P. E. Wright, and M. Rance, Sensitivity improvement in proton-detected two-dimensional heteronuclear correlation NMR spectroscopy, *J. Magn. Reson.* **93,** 151–170 (1991).
30. R. R. Ernst, G. Bodenhausen, and A. Wokaun, "Principles of Nuclear Magnetic Resonance in One and Two Dimensions," Clarendon Press, Oxford, 1987.
31. S. Berger, Selective inverse correlation of ^{13}C and ^{1}H NMR signals, an alternative to 2D NMR, *J. Magn. Reson.* **81,** 561–564 (1989).